Climate of the Past Discussions

Climate of the Past Discussions is the access reviewed discussion forum of *Climate of the Past*

Title Page

Abstract | Introduction

Conclusions | References

Tables | Figures

|◄ | ►|

◄ | ►

Back | Close

Full Screen / Esc

Printer-friendly Version

Interactive Discussion

EGU

South Atlantic island record reveals a South Atlantic response to the 8.2 kyr event

K. Ljung[1], S. Björck[1], H. Renssen[2], and D. Hammarlund[1]

[1]Geobiosphere Science Centre, Department of Geology, Quaternary Sciences, Lund University, Sölvegatan 12, 223 62 Lund, Sweden
[2]Faculty of Earth and Life Sciences, Vrije Universiteit Amsterdam, De Boelelaan 1085, 1081 HV Amsterdam, Netherlands

Correspondence to: K. Ljung (karl.ljung@geol.lu.se)

Abstract

One of the most distinct climate fluctuations during the Holocene is the short and rapid event centred around 8200 years ago, the 8.2 kyr event, which was most likely triggered by glacial melt-water forcing from the receding Laurentide ice-sheet. Evidence for this cooling has primarily been reported from sites around the North Atlantic, but an increasing number of observations imply a more wide-spread occurrence. Palaeoclimate archives from the Southern Hemisphere have hitherto failed to uncover a distinct climatic anomaly associated with the 8.2 kyr event. Here we present a lake sediment record from Nightingale Island in the central South Atlantic showing enhanced precipitation between 8275 and 8025 cal. yrs BP, most likely as a consequence of increased sea surface temperature (SST). We show that this is consistent with climate model projections of a warming of the South Atlantic in response to reduced north-ward energy transport during the 8.2 kyr event.

1 Introduction

The cooling associated with the 8.2 kyr event (Alley et al., 1997) is commonly attributed to a weakening of the North Atlantic Deep Water (NADW) formation by rapid discharge of melt-water from ice-dammed lakes to the North Atlantic Ocean from the margin of the Laurentide Ice Sheet (Barber et al., 1999). Evidence for this cooling has primarily been reported from sites around the North Atlantic, but an increasing number of observations imply a more wide-spread occurrence (Alley and Ágústsdóttir, 2005; Rohling and Pälike, 2005; Wiersma and Renssen, 2006). Coupled atmosphere-ocean model results (Bauer et al., 2004; LeGrande et al., 2006; Renssen et al., 2002; Renssen et al., 2001) indicate that such freshening of the North Atlantic caused a significant decrease in the north-ward heat transport, leading to a warming of the South Atlantic, and resulting in increased SST and precipitation in the South Atlantic as a response to the weakened thermohaline circulation (THC). Therefore this is a key region for in-

South Atlantic 8.2 kyr event

K. Ljung et al.

EGU

vestigating the climatic signature and extent of the 8.2 kyr event, for testing the climate models, and any Holocene anti-phase behavior of north and south (Crowley, 1992; Stocker et al., 1992), the so-called bipolar seesaw effect (Broecker, 1998; Stocker, 1998). Although a relationship between seesawing and ice-rafting (IRD) events in the
5 North Atlantic has been hypothesized (Broecker et al., 1999), no records with a clear anti-phase response to the 8.2 kyr event, or other IRD events, have been found (Morrill and Jacobsen, 2005). Marine records from the South Atlantic (Piotrowski et al., 2004) and Tropical Atlantic (Arz et al., 2001) imply a weakening of NADW formation around 8000 cal. yrs BP, without a seesaw effect, while other South Atlantic records show no
10 changes during this time (Nielsen et al., 2004).

The Tristan da Cunha island group is located at 37° S in the central South Atlantic (Figs. 1a and b), in the path of the westerlies at the northern limit of the West Wind Drift, and has a climate sensitive to atmospheric and oceanographic changes. Mean annual temperature is 14°C and annual precipitation close to sea level at The Settlement is ca.
15 1500 mm, while values three times higher have been indicated for the more elevated parts of the island. Abundant peat and lake deposits on the islands provide targets for studies of past hydrological changes (Ljung et al., 2006).

We retrieved a 9.6 m long sediment sequence from the central part of an overgrown lake on the small (3.2 km^2) Nightingale Island (Fig. 1c, Fig. 2). This fen, situated at
20 ca. 180 m above sea level, is called 2nd Pond and has a size of ca. 1 ha. It is a distinct basin with no in- or outlets. *Scirpus* sp. and *Sphagnum* sp. dominate the fen vegetation, while thick tussock-grass dominated by *Spartina arundinaceae* and *Poa flabellata* cover most of the island. Trees *(Phylica arborea)*, tree ferns *(Blechnum palmiforme)* and associated shade-tolerant species *(Nertera* sp., Polypodiaceae) are
25 restricted to slopes and higher areas.

Here we present a palaeoclimatic reconstruction based on a multi-proxy study, including magnetic susceptibility, pollen analysis, and determination of total carbon (TC), nitrogen (TN) and sulphur (TS) content, of the lower part of this sequence, which covers the time period 10 700 to 7000 cal. yrs BP (Figs. 2 and 3). The emphasis is on

the 8.2 kyr event, which is distinctly expressed in the sequence, and its coupling to the Atlantic Ocean circulation. We compare our results with a simulation of the 8.2 kyr BP event performed with a coupled atmosphere-ocean climate model.

2 Methods

2.1 Coring, lithological descriptions and correlations

The sediment sequence was recovered with a 5 cm Russian chamber corer. All cores were visually described in the field and in detail in the laboratory. Special attention was paid to any signs of potential volcanic ash layers (tephras). Correlations between overlapping cores were carried out visually and with the aid of magnetic susceptibility measurements.

2.2 Radiocarbon dating

The chronology is based on ^{14}C measurements performed at the Compact Carbon AMS laboratory in Poznan, Poland, and the Single Stage AMS laboratory in Lund, Sweden. The measurements were obtained on macroscopic plant remains and bulk sediment samples. Radiocarbon ages were converted to calibrated ages using the program OxCal v3.10 (Bronk Ramsey, 1995, 2001) and the SHCal04 calibration dataset (McCormac et al., 2004). The age model was constructed by visually fitting lines through the calibrated radiocarbon dates, and adjusting sedimentation rate changes according to the lithology and lithologic changes displayed in the sequence.

2.3 Total carbon, nitrogen and sulphur measurements

Total carbon, nitrogen and sulphur were obtained on dried and homogenized samples using a Costech Instruments ECS 4010 elemental analyzer. Measurement accuracy

EGU

is better than ±5% of the reported values based on replicated standard samples. C/N atomic ratios were obtained by multiplying by 1.67 (Bengtsson and Enell, 1986).

If no inorganic carbon, i.e. no carbonates, are present, TC and TN contents are directly related to organic matter content, and the C/N ratio can be used to asses the proportion of terrestrial versus aquatic organic matter in the sediments (Meyers and Teranes, 2001).

2.4 Magnetic susceptibility measurements

Magnetic susceptibility was measured at 4 mm increments using a Bartington Instruments MS2EI magnetic susceptibility high-resolution surface scanning sensor coupled to a TAMISCAN automatic logging conveyor. Magnetic susceptibility reflects the minerogenic content of the sediments and provides a proxy for in-wash from the catchment (Thompson and Oldfield, 1986).

2.5 Pollen analysis

Pollen samples of c. 1 cm^3 were processed following standard method A (Berglund and Ralska-Jasiewiczowa, 1986), with added Lycopodium spores. The counting was made under a light microscope at magnifications of ×400 and ×1000. Pollen grains were identified by the help of published photos (Hafsten, 1960), standard pollen keys (Moore et al., 1991), and a small collection of type slides prepared by U. Hafsten and borrowed from the Botanical Museum in Bergen, Norway. Zonation of the pollen diagram is based on the variation of the major taxa and follows the result from the principal component analysis.

2.6 Principal component analysis

Principal component analysis (PCA) was performed in MATLAB using the function princomp. Undetermined pollen grains were excluded from the analysis. The percentage

EGU

data were normalized and standardized prior to analysis. PCA was used to extract the major variation from the total pollen percentage dataset.

2.7 Climate model and experimental design

We have performed the simulation of the 8.2 kyr event with version 2 of the ECBilt-CLIO coupled atmosphere-ocean model. The atmospheric component is ECBilt, an atmospheric model (T21 horizontal resolution, three layers) based on quasi-geostrophic equations (Opsteegh et al., 1998). As an extension to the quasi-geostrophic equations, an estimate of the neglected terms in the vorticity and thermodynamic equations is included as a temporally and spatially varying forcing. This forcing is calculated from the diagnostically derived vertical motion field and leads to a considerable improvement of the simulation of the Hadley Cell circulation, resulting in a better representation of the strength and position of the jet stream and transient eddy activity. ECBilt resolves synoptic variability associated with weather patterns. ECBilt is coupled to CLIO, an oceanic general circulation model (3°×3° latitude-longitude horizontal resolution, 19 layers in the vertical) coupled to a comprehensive dynamic-thermodynamic sea-ice model (Goosse and Fichefet, 1999). The ECBilt-CLIO model reproduces the modern climate (Goosse et al., 2001; Renssen et al., 2002) reasonably well.

The simulation experiment on the 8.2 kyr event was designed as follows. First, starting from a modern quasi-equilibrium state, the model was run for 550 years with forcings for 8.5 kyr BP to obtain an early Holocene climate state (Renssen et al., 2002). These forcings are orbital parameters (Berger, 1978), greenhouse gas concentrations (Raynaud et al., 2000), modified surface albedo in northern Africa to account for a "green" Sahara (Adams and Fauré, 1997), and modified surface albedo and surface elevation in North America to represent the remnant Laurentide Ice Sheet (Peltier, 1994). At the end of the 550 years, the trend in the global ocean temperature was only –0.007°C/century. Second, this 8.5 kyr BP early Holocene quasi-equilibrium state was perturbed by releasing a freshwater pulse in the Labrador Sea that represents the catastrophic drainage from Lakes Agassiz and Ojibway and the collapse of the Lauren-

EGU

tide Ice Sheet Dome over the Hudson Bay. Different freshwater volumes and release rates were tested (Renssen et al., 2002). After the introduction of the freshwater perturbations, the experiments were continued for at least 500 years. Here we present results from one particular experiment that produced a climate anomaly that was clos-
est to what is suggested by proxy data on the 8.2 kyr event, both in terms of magnitude and duration (Renssen et al., 2002; Wiersma and Renssen, 2006). In this experiment, we released a constant freshwater flux of 0.75 Sv (1 Sv = 1×10^6 m^3/s) in the Labrador Sea during 20 years, implying a total volume of 4.67×10^{14} m^3. This freshwater volume is close to the highest estimate for the 8.2 kyr event based on geological data (Von
Grafenstein et al., 1999).

3 Results

3.1 Chronology and climate reconstruction

The depth-age relationship of the lowermost 2.5 m was determined by 22 ^{14}C measurements (Fig. 2, Table 1). The results from this part of the sequence, covering the
time period from 10 750 to 7000 cal. yrs BP, are presented in Figs. 2 and 3. The temporal resolution of the magnetic susceptibility data is ca. 10 years, equivalent to the geochemical data for the period 8300–7500 cal. yrs BP. The rest of the geochemical record has ca. 20 year resolution, although the pollen record is of lower resolution (30–60 years at 8600–7400 cal. yrs BP and 70–150 years in the oldest part of the
sequence). We estimate that the age envelope of the age model is at least ±25 years.
The lower part of the sediment sequence consists of bog peat with a variable degree of humification (Fig. 2). The peat is overlain by lacustrine sediments (gyttja) with low minerogenic content, with this gradual transition at 8.7–8.6 m dated to 8800–8600 cal. yrs BP. The highly organic gyttja is interspersed with distinct units of silty
gyttja at 8.33–8.09 m and at 7.65–7.55 m. In this volcanic bedrock region the minerogenic content of the sediments is mirrored by the magnetic susceptibility values, and

K. Ljung et al.

Title Page

Abstract | Introduction

Conclusions | References

Tables | Figures

◄◄ | ►►

◄ | ►

Back | Close

Full Screen / Esc

Printer-friendly Version

Interactive Discussion

EGU

closely follows the lithological changes. In the lowermost peat (9.7–8.7 m) the magnetic susceptibility is very low and remains low after the transition to gyttja. The exception is a temporary susceptibility increase at ca. 8550 cal. yrs BP (Fig. 3), which is likely related to in-wash processes connected to the bog-to-lake transition. Within the two silty gyttja units at 8.33–8.09 m and 7.65–7.55 m (Fig. 3), magnetic susceptibility increases markedly. The lower of these units was dated to 8275–8025 cal. yrs BP, making it synchronous with the Northern Hemisphere 8.2 kyr event (Alley et al., 1997). The upper silty gyttja unit is dated to 7500–7300 cal. yrs BP (Fig. 3).

Total carbon content of the peat and the overlying gyttja ranges from 40 to 45%, which corresponds to at least 80–90% organic matter due to absence of inorganic carbon (Fig. 3). During the increase in minerogenic matter at 8275–8025 cal. yrs BP, total carbon content drops to 16%, and at 7500–7300 cal. yrs BP a minimum of 15% is reached. TC/TN ratios of the fen peat generally exceed 40 with a maximum above 80, which indicates dominance of terrestrial organic matter (Meyers, 2003). TC/TN ratios in the range of 20–30 characterize the lacustrine part of the sequence, with higher values at 8275–8025 and 7500–7300 cal. yrs BP.

The pollen data show large variations which generally follow the lithological changes and variations in the other proxies (Fig. 4). Principal component analysis (PCA) was used to extract the major variation in the pollen percentage data (Fig. 5). The first two axes explain 33% and 19% of the total variance, respectively. The first axis values are primarily determined by Cyperaceae, having the highest scores, and *Phylica arborea, Acaena* sp., Polypodiaceae, *Empetrum rubrum*, Gramineae, Chenopodiaceae and *Rumex frutescens*, which have the lowest (negative) scores. The second axis values are primarily driven by the low negative scores of *Callitriche christensenii* and the high positive scores of *Lycopodium insulare*. These two PCA axes divide the pollen assemblage into different habitat groups: the 1st axis separates local littoral vegetation (Cyperaceae and *Callitriche christensenii*), dominating pollen zones 2, 4 and 6, from more distal catchment taxa (*Phylica arborea*, *Empetrum rubrum*, *Acaena* sp., *Rumex frutescens* and Polypodiaceae), dominating pollen zones 3 and 5, whilst the 2nd axis

South Atlantic 8.2 kyr event

K. Ljung et al.

EGU

separates the typical bog species *Lycopodium insulare* , present in pollen zone 1, from the aquatic species *Callitriche christensenii*, present in pollen zones 2–6. The 1st axis sample scores are closely correlated with TC content (r=0.8, *P*<0.001), TN content (r=0.6, *P*<0.001) and magnetic susceptibility (r=0.8, p<0.001).

3.2 Model results

In our experiment of the 8.2 kyr event there is a clear increase in relative humidity over the SE Atlantic as a response to the North Atlantic THC weakening, as well as higher SST's (Fig. 6). This is especially evident during August–October, which is the period with the largest increases in temperature and precipitation in the model. This confirms that in our model the precipitation increases are related to higher SST's, following the principle: warmer surface ocean, more evaporation, higher air humidity, more precipitation.

It should be noted that, when compared to comprehensive coupled GCMs, our model of intermediate complexity simulates a weak response of the hydrological cycle to a THC weakening. We have chosen to use a model of intermediate complexity for our study on the 8.2 kyr event because this has enabled us to perform a range of multi-centennial runs to test different freshwater scenarios (Renssen et al., 2002). These experiments would not have been feasible with coupled GCMs. As presented in the recent model-intercomparison by Stouffer et al. (2006), coupled GCMs simulate a pronounced southward shift in the ITCZ over the South Atlantic as a response to a THC perturbation, a response that is underestimated in our model. However, the GCM results show that the precipitation increase that is associated with this southward ITCZ shift is restricted to the latitudinal band ranging from 0 to 30° S, so considerably north of Nightingale Island (at about 37° S). However, the coupled GCMs show a secondary precipitation increase over the South Atlantic between 35 and 40° S as a response to the THC weakening. This secondary precipitation maximum is modest (about +11% in their 1 Sv perturbation runs) compared to the primary precipitation maximum associated with the ITCZ shift (up to +100% in the 1 Sv perturbation runs). Stouffer et

South Atlantic 8.2 kyr event

K. Ljung et al.

EGU

al. (2006) provide no explanation for this secondary precipitation maximum, but it is noteworthy that in the GCMs the ocean surface is considerably warmer at this latitude in the South Atlantic, so that it is likely that there is a link (higher precipitation due to higher SST) as is also seen in our model results.

4 Discussion

The pattern in most of our proxy records can be explained in terms of variations in effective humidity and precipitation. The basal peat indicates an at least 9 m lower water table than at present. The bog-to-lake transition must be the result of significantly increased effective humidity. This implies that a major change of the general circulation pattern took place around 8800 cal. yrs BP, likely reflecting the establishment of the present-day circulation regime, due to a meridional shift of the regional fronts. In fact, marine studies in the Atlantic sector of the Southern Ocean (Nielsen et al., 2004) and land-based studies in South America imply that the westerlies intensified after 9000 cal. yrs BP (Mayr et al., 2007). Temperature reconstructions from Antarctic ice cores show that the Holocene thermal optimum came to an end at about this time (Epica community members, 2004; Masson et al., 2000) (Fig. 3), which resulted in expanded sea ice cover and steeper meridional temperature gradient in the Southern Ocean. Model studies have shown that changes in sea ice extent also causes corresponding changes in the position of the westerlies (Hudson and Hewitson, 2001). Thus, it is likely that the westerlies strengthened and shifted northwards in the South Atlantic region at the end of the Antarctic thermal optimum around 9000–8500 cal. yrs BP, as a result of increased meridional temperature gradient and expanded sea ice. The change from peat growth to gyttja deposition and declining bog species and the appearance of aquatic species in the pollen diagram represented by lower values on the 2nd PCA axis (Fig. 3), are direct effects of this precipitation increase.

At 8275 cal. yrs BP we note enhanced influx of minerogenic and terrestrial organic matter, and increased deposition of pollen types from more remote parts of the catch-

South Atlantic 8.2 kyr event

K. Ljung et al.

|◄   ►|

◄   ►

Back   Close

Full Screen / Esc

Printer-friendly Version

Interactive Discussion

EGU

ment. We believe that these simultaneous changes in lithology, minerogenic content, TC/TN ratio and pollen content (Fig. 3) could only have been caused by increased surface run-off in response to increased precipitation. This led to increased catchment erosion and higher input of terrestrial detritus to the basin. This also explains the simultaneous increase in pollen from taxa favoured by open ground, such as *Rumex frutescens* , and closed forest species, such as *Phylica arborea*. It is unlikely that this pollen assemblage change represents a true vegetation change since an expansion of forest would limit open ground taxa and vice versa. Therefore we conclude that the stratigraphic changes at 8275–8025 cal. yrs BP reflect a period of increased precipitation on Nightingale Island.

At present, stronger westerlies or higher SSTs, the latter generating increased air humidity, are the main agents behind enhanced precipitation in the study area. So, which of these possible mechanisms triggered the changes we see? Intensified westerlies are connected to higher wind speeds, resulting in increased concentrations of sea spray, with sea salt sulphates as one important marine aerosol component in coastal areas. We note the low TS values (Fig. 3) at this time, which can be explained as both an effect of lower organic carbon content and lower sulphur concentrations in the aerosols. Furthermore, the higher TC/TS values show that the relative decline in TS content was larger than that of TC. This is a strong indication that concentrations of sea salt sulphates in the aerosols of Nightingale Island were not higher, but rather lower, during the stratigraphic changes at 8275–8025 cal. yrs BP. We therefore hypothesize that the increase in evaporation was caused by higher SST's.

The age of 8275–8025 cal. yrs BP for the inferred precipitation increase at 8.33–8.09 m is firmly established by the radiocarbon dates and allows for detailed correlation with other climate archives. The onset of changes is coeval with the onset of the 8.2 kyr event in the new NGRIP ice core, where it is dated to 8260 cal. yrs BP (Rasmussen et al., 2006), as well as with the shift in the Cariaco Basin grey scale record (Hughen et al., 2000), dated to 8290 cal. yrs BP (Fig. 3), and with the inferred decline in North Atlantic meridional overturning circulation at 8290 cal. yrs BP (Ellison et al.,

EGU

2006). The inferred increase in precipitation at 8275–8025 cal. yrs BP is consistent with different model simulations of the 8.2 kyr event (Bauer et al., 2004; LeGrande et al., 2006; Renssen et al., 2002; Renssen et al., 2001). Our coupled atmosphere-ocean model simulations show statistically significant (at 95% level) increases in SST (by 0.2

5 to 0.5°C in annual mean) and precipitation (by 10 to 60 mm/yr in annual mean) over the South Atlantic in response to a freshwater-induced weakening of the THC (Wiersma and Renssen, 2006) (Fig. 6). In the model, the warming is related to reduced northward heat transport in the Atlantic Ocean, causing heat to accumulate in the South Atlantic, the so-called bipolar seesaw effect, and the warmer surface waters in turn

10 stimulate precipitation in the study region. These model results support our hypothesis that higher SSTs triggered the increased precipitation at our site. Furthermore, the increase in precipitation over Nightingale Island as a response of a warmer ocean was probably stronger than suggested by the model (Fig. 6), as the local topography of the >300 m high island causes forced lifting of passing air masses, resulting in distinctly

15 higher precipitation than modeled. The model also shows that the westerlies were not strengthened over the South Atlantic during the 8.2 kyr event. Thus the increase in precipitation at 8275–8025 cal. yrs BP is not only coeval with the 8.2 ka event but also shows the response predicted by our climate model (Fig. 6). We therefore conclude that this change is the South Atlantic expression of the 8.2 ka event.

20 Our data do not show any indication of a supposed general climate anomaly starting at 8500 cal. yrs BP and lasting 500–700 years (Keigwin et al., 2005; Rohling and Pälike, 2005), but only register the more restricted 8.2 kyr event. The duration of the event in our record is approximately 250 years, which is longer than the 160–180 years of the 8.2 kyr event in the NGRIP (Rasmussen et al., 2006) and Cariaco Basin records

25 (Hughen et al., 2000). If this anomaly is correct it may possibly be explained by the thermal inertia of the ocean.

The very similar changes in proxy data at 7500–7300 cal. yrs BP compared to those at 8275–8025 kyr BP (Fig. 3) indicate that this period was also characterized by increased precipitation. This implies that these periods of increased precipitation were

EGU

not unique, but are part of a pattern of recurring Holocene events. It is therefore note-worthy that our event at 7500-7300 kyr BP coincides with one of the most distinct Holocene North Atlantic IRD peaks/^{14}C production maxima (Bond et al., 2001). Fur-thermore, in spite of a different hydrological regime before 8800 cal. yrs BP, with peat accumulation instead of lake sedimentation, we note that our pollen data display two peaks in the 2nd axis *PC* values (Fig. 3), which are caused by high frequencies of the bog species *Lycopodium insulare* . The uppermost of these peaks also coincides with a period of lower humified peat. Thus, these two periods represents wetter conditions at the bog. The two periods are separated by high *Phylica arborea* and Polypdiaceae frequencies, and high content of *Blechnum palmiforme* remains, which indicates a drier tree covered bog surface. The two wetter periods are dated to 10 300–10 500 and 9600–9700 cal. yrs BP, respectively, and thus coincides with two cold phases in the Atlantic region (Björck et al., 2001; Bond et al., 2001). We also note that several lithological changes similar to the ones at 8275–8025 and 7500–7300 cal. yrs BP oc-cur throughout the rest of the core. This implies that the 8.2 kyr event was not the only period of increased precipitation on Nightingale Island during the Holocene, and it may suggest that changes in the meridional overturning circulation was a recurring phenomenon throughout the Holocene. This is in agreement with the variable Atlantic circulation inferred from marine sediment cores (Bond et al., 2001).

It has been shown that NADW formation and the strength of THC have varied throughout the Holocene and that a weakened THC during the 8.2 kyr event was only one of several similar events (Hall et al., 2004; Oppo et al., 2003). This scenario is sup-ported by our data, although it may be difficult to comprehend why large-scale glacial lake drainage did not perturb the THC significantly more than at other periods of weak THC. One explanation may be that the 8.2 kyr event is an anomaly with a different trig-gering mechanism, as compared to most of the other Holocene events, where solar forcing and related feedbacks have been invoked as major players (Bond et al., 2001).

EGU

5 Conclusions

The results show that our island paleoclimate record from the central South Atlantic responded to the North Atlantic 8.2 kyr BP cooling with an increase in precipitation. This was most likely caused by increased SSTs in the surrounding ocean, which is also demonstrated by modelling the coupled atmosphere-ocean response to an 8.2 kyr BP freshwater pulse into the North Atlantic. This is the first clear demonstration of a climatic response in the South Atlantic to the 8.2 kyr BP event, and it shows that the disruption of NADW formation caused by the drainage of the Laurentide ice-dammed lakes also affected the central South Atlantic.

References

Adams, J. M. and Fauré, H.: Review and Atlas of Palaeovegetation: Preliminary land ecosystem maps of the world since the Last Glacial Maximum. Oak Ridge National Laboratory, TN, USA, 1997.

Alley, R. B. and Ágústsdóttir, A. M.: The 8 k event: cause and consequences of a major Holocene abrupt climate change, Quat. Sci. Rev. 24, 1123–1149, 2005.

Alley, R. B., Mayewski, P. A., Stuiver, M., Taylor, K. C., and Clark, P. U.: Holocene climatic instability: A prominent, widespread event 8200 yr ago, Geology, 25, 483–486, 2007.

Arz, H. W., Gerhardt, S., Pätzold, J., and Röhl, U.: Millennial-scale changes of surface- and deep-water flow in the western tropical Atlantic linked to Northern Hemisphere high-latitude climate during the Holocene, Geology, 29, 239–242, 2001.

Barber, D. C., Dyke, A., Hillaire-Marcel, C., Jennings, A. E., Andrews, J. T., Kerwin, M. W., Bilodeau, G., McNeely, R., Southon, J., Morehead, M. D., and Gagnon, J. M.: Forcing of

South Atlantic 8.2 kyr event

K. Ljung et al.

⏮ | ⏭

◀ | ▶

Back | Close

Full Screen / Esc

Printer-friendly Version

Interactive Discussion

EGU

the cold event of 8200 years ago by catastrophic drainage of Laurentide lakes, Nature, 400, 344–348, 1999.

Bauer, E., Ganopolski, A., and Montoya, M.: Simulation of the cold climate event 8200 years ago by meltwater outburst from Lake Agassiz, Paleoceanography, 19, PA001030, doi:10.1029/2004PA001030, 2004.

Bengtsson, L. and Enell, M.: Chemical analysis, in: Handbook of Holocene Palaeoecology and Palaeohydrology, edited by: Berglund, B. E., Jhon Wiley & Sons Ldt, Chichester, 423–451, 1986.

Berger, A. L.: Long-term variations of daily insolation and Quaternary climatic changes, J. Atmos. Sci., 35, 2363–2367, 1978.

Berglund, B. E., and Ralska-Jasiewiczowa, M.: Pollen analysis and pollen diagrams, in: Handbook of Holocene palaeoecology and palaeohydrology, edited by: Berglund, B. E., Wiley, Chichester, 455–484, 1986.

Björck, S., Muscheler, R., Kromer, B., Andresen, C. S., Heinemeier, J., Johnsen, S. J., Conley, D., Koç, N., Spurk, M., and Veski, S.: High-resolution analyses of an early Holocene climate event may imply decreased solar forcing as an important climate trigger, Geology, 29, 1107–1110, 2001.

Bond, G., Kromer, B., Beer, J., Muscheler, R., Evans, M. N., Showers, W., Hoffman, S., Lotti-Bond, R., Hajdas, I., and Bonani, G.: Persistent solar influence on North Atlantic climate during the Holocene, Science, 294, 2130–2136, 2001.

Broecker, W. S.: Paleocean circulation during the last deglaciation: A bipolar seesaw?, Paleoceanography, 13, 119–121, 1998.

Broecker, W. S., Sutherland, S., and Tsung-Hung, P.: A possible 20th-century slowdown of southern ocean deep water formation, Science, 286, 1132–1135, 1999.

Bronk Ramsey, C.: Radiocarbon calibration and analysis of stratigraphy: The OxCal program, Radiocarbon, 37, 425–430, 1995.

Bronk Ramsey, C.: Development of the radiocarbon program OxCal, Radiocarbon, 43, 381–389, 2001.

Crowley, T. J.: North Atlantic deep water cools the Southern Hemisphere, Paleoceanography, 7, 489–497, 1992.

Ellison, C. R. W., Chapman, M. R., and Hall, I. R.: Surface and deep ocean interactions during the cold climate event 8200 years ago, Science, 312, 1929–1932, 2006.

Epica community members.: Eight glacial cycles from an Antarctic ice core, Nature, 429, 623–

South Atlantic 8.2 kyr event

K. Ljung et al.

EGU

628, 2004.

Goosse, H. and Fichefet, T.: Importance of ice-ocean interactions for the global ocean circulation: a model study, J. Geophys. Res., 104, 23 337–23 355, 1999.

Goosse, H., Selten, F. M., Haarsma, R. J., and Opsteegh, J. D.: Decadal variability in high northern latitudes as simulated by an intermediate-complexity climate model, Ann. Glac., 33, 525–532, 2001.

Hafsten, U.: Pleistocene development of vegetation and climate in Tristan da Cunha and Gough Island. Arbok Univeristetet i Bergen, Mat.-Naturv. Serie. A, 20, 1–45, 1960.

Hall, I. R., Bianchi, G. G., and Evans, J. R.: Centennial to millennial scale Holocene climate-deep water linkage in the North Atlantic, Quat. Sci. Rev., 23, 1529–1536, 2004.

Haug, G. H., Hughen, K. A., Peterson, L. C., Sigman, D. M., and Rohl, U.: Southward migration of the Intertropical Convergence Zone through the Holocene, Science, 293, 1304–1308, 2001.

Hudson, D. A. and Hewitson, B. C.: The atmospheric response to a reduction in summer Antarctic sea-ice extent, Clim. Res., 16, 76–99, 2001.

Hughen, K. A., Southon, J. R., Lehman, S., and Overpeck, J.: Synchronous radiocarbon and climate shifts during the last deglaciation, Science, 290, 1951–1955, 2000.

Keigwin, L. D., Sachs, J. P., Rosenthal, Y., and Boyle, E. A.: The 8200 year B.P. event in the slope water system, western subpolar North Atlantic, Paleoceanography, 20, PA001074, doi:10.1029/2004PA001074, 2005.

LeGrande, A. N., Schmidt, G. A., Shindell, D. T., Field, C. V., Miller, R. L., Koch, D. M., Faluvegi, G., and Hoffman, G.: Consistent simulations of multiple proxy responses to an abrupt climate change event, Proc. Natl. Acad. Sci., 103, 837–842, 2006.

Ljung, K., Björck, S., Hammarlund, D., and Barnekow, L.: Late Holocene multi-proxy records of environmental change on the South Atlantic island Tristan da Cunha, Palaeogeogr. Palaeoclim. Palaeoecol., 241, 539–560, 2006.

Masson, V., Vimeux, F., Jouzel, J., Morgan, V., Delmotte, M., Ciais, P., Hammer, C., Johnsen, S., Lipenkov, V. Y., Mosley-Thompson, E., Petit, J.-R., Steig, E. J., Stievenard, M., and Vaikmae, R.: Holocene Climate Variability in Antarctica Based on 11 Ice-Core Isotopic Records, Quat. Res. 54, 348–358, 2000.

Mayr, C., Wille, M., Haberzettl, T., Fey, M., Janssen, S., Lücke, A., Ohlendorf, C., Oliva, G., Schäbitz, F., Schleser, G. H., and Zolittschka, B.: Holocene variability of the Southern Hemisphere westerlies in Argentinean Patagonia (52S), Quat. Sci. Rev., 26, 579–584, 2007.

South Atlantic 8.2 kyr event

K. Ljung et al.

Title Page

Abstract	Introduction
Conclusions	References
Tables	Figures

◄◄	►►
◄	►
Back	Close

Full Screen / Esc

Printer-friendly Version

Interactive Discussion

EGU

McCormac, F. G., Hogg, A. G., Blackwell, P. G., Buck, C. E., Higham, T. F. G., and Reimer, P. J.: SHCal04 Southern Hemisphere Calibration, 0 - 11 kyr cal BP, Radiocarbon, 46, 1087–1092, 2004.

Meyers, P. A.: Applications of organic geochemistry to paleolimnological reconstructions: a summary of examples from the Laurentian Great Lakes, Org. Geochem., 34, 261–289, 2003.

Meyers, P. A. and Teranes, J. L.: Sediment organic matter, in: Tracking environmental cange using lake sediments, edited by: Last, W. M. and Smol, J. P., Kluwer Academic Publishers, Dordrecht, 239–269, 2001.

Moore, P. D., Webb, J. A., and Collinson, M. E.: Pollen analysis. Blackwell Scientific, Oxford, 1991.

Morrill, C. and Jacobsen, R. M.: How widespread were the climate anomalies 8200 years ago?, Geophys. Res. Lett., 32, L19701, doi:10.1029/2005GL023536, 2005.

Nielsen, S. H. H., Koc, N., and Crosta, X.: Holocene climate in the Atlantic sector of the Southern Ocean: controlled by insolation or oceanic circulation?, Geology, 32, 317–320, 2004.

Oppo, D. W., McManus, J. F., and Cullen, J. L.: Deepwater variability in the Holocene epoch, Nature, 422, 277–279, 2003.

Opsteegh, J. D., Haarsma, R. J., Selten, F. M., and Kattenberg, A.: ECBILT: a dynamic alternative to mixed boundary conditions in ocean models, Tellus 50A, 348–367, 1998.

Peltier, W. R.: Ice age paleotopography, Science, 265, 195–201, 1994.

Piotrowski, A. M., Goldstein, S. L., Hemming, S. R., and Fairbanks, R. G.: Intensification and variability of ocean thermohaline circulation through the last deglaciation, Earth Planet. Sci. Lett., 225, 205–220, 2004.

Rasmussen, S. O., Andersen, K. K., Svensson, A. M., Steffensen, J. P., Vinther, B. M., Clausen, H. B., Siggaard-Andersen, M.-L., Johnsen, S. J., B., L. L., Dahl-Jensen, D., Bigler, M., Röthlisberger, R., Fischer, H., Goto-Azuma, K., Hansson, M. E., and Ruth, U.: A new Greenland ice core chronology for the last glacial termination, J. Geophys. Res., 111, D06102, doi:10.1029/2005JD006079, 2006.

Raynaud, D., Barnola, J.-M., Chappellaz, J., Blunier, T., Indermühle, A., and Stauffer, B.: The ice record of greenhouse gases: a view in the context of future changes, Quat. Sci. Rev., 19, 9–17, 2000.

Renssen, H., Goosse, H., and Fichefet, T.: Modelling the effect of freshwater pulses on the early Holocene climate: the influence of high-frequency climate variability, Paleoceanography, 17, PA000649, doi:10.1029/2001PA000649, 2002.

EGU

Renssen, H., Goosse, H., Fichefet, T., and Campin, J.-M.: The 8.2 kyr event simulated by a global atmosphere-sea-ice-ocean model, Geophys. Res. Lett., 28, 1567–1570, 2001.

Rohling, E. J. and Pälike, H.: Centennial-scale climate cooling with a sudden cold event around 8200 years ago, Nature, 434, 975–979, 2005.

Röthlisberger, R., Mulvaney, R., Wolff, E. W., Hutterli, M. A., Bigler, M., Sommer, S., and Jouzel, J.: Dust and sea-salt variability in central East Antarctica (Dome C) over the last 45 kyrs and its implications for southern high-latitude climate, Geophys. Res. Lett., 29, 1963, 2002.

Stocker, T. F.. The seesaw effect, Science, 282, 61–62, 1998.

Stocker, T. F., Wright, D. G., and Mysak, L. A.: A zonally averaged, coupled ocean-atmosphere model for paleoclimate studies, J. Climate, 5, 773–797, 1992.

Stouffer, R. J.: Investigating the causes of the response of the thermohaline circulation to past and future climate changes, J. Climate, 19, 1365–1387, 2006.

Thompson, R. and Oldfield, F.: Environmental magnetism. Allen & Unwin, London, 1986.

Wiersma, A. P. and Renssen, H.: Model-data comparison for the 8.2ka BP event: confirmation of a forcing mechanism by catastrophic drainage of Laurentide Lakes, Quat. Sci. Rev., 25, 63–88, 2006.

Von Grafenstein, U., Erlenkeuser, H., Brauer, A., Jouzel, J., and Johnsen, S. J.: A mid-European decadal isotope-climate record from 15 500 to 5000 years BP, Science, 284, 1654–1657, 1999.

South Atlantic 8.2 kyr event

K. Ljung et al.

Title Page

Abstract | Introduction

Conclusions | References

Tables | Figures

◄ | ►

◄ | ►

Back | Close

Full Screen / Esc

Printer-friendly Version

Interactive Discussion

EGU

Table 1. Radiocarbon dates from the 2nd Pond sequence between 9.635 and 7.04 m below the fen surface.

| Lab. Nr	Depth (cm)	^{14}C Age	Cal. yr BP (2σ)	Dated material
LuS-5799	704	6220±50	7074.5±175	Bulk sediment
LuS-6688	733	6215±60	7069.5±180	Terrestrial macrofossils
LuS-5812	747.5	6365±50	7219.5±200	Terrestrial macrofossils
LuS-5800	747.5	6560±50	7424.5±135	Bulk sediment
LuS-6231	766.5	6950±60	7769.5±160	Terrestrial macrofossils
LuS-6689	775.5	6790±50	7589.5±90	Terrestrial macrofossils
LuS-5813	802	7105±50	7859.5±120	Terrestrial macrofossils
LuS-5801	802	7115±50	7874.5±125	Bulk sediment
LuS-6230	812.5	7360±50	8139.5±160	Terrestrial macrofossils
LuS-6229	822.5	7410±50	8169.5±150	Terrestrial macrofossils
LuS-6406	829	7350±60	8129.5±170	Terrestrial macrofossils
LuS-6228	833	7665±50	8444.5±105	Terrestrial macrofossils
LuS-6407	835.5	7620±60	8354.5±165	Terrestrial macrofossils
LuS-5814	844	7310±50	8074.5±105	Terrestrial macrofossils
LuS-5802	844	7605±100	8359.5±200	Bulk sediment
LuS-6690	863.5	7725±50	8484.5±105	Terrestrial macrofossils
LuS-5815	875.5	8080±50	8834.5±195	Terrestrial macrofossils
Lus-5803	875.5	8185±60	9024.5±275	Bulk sediment
Poz-4444	912	8720±50	9654.5±135	Terrestrial macrofossils
Poz-4488	945.25	9120±190	10149.5±600	Terrestrial macrofossils
Poz-4941	962.25	9460±50	10634.5±145	Terrestrial macrofossils
Poz-4489	963.5	8760±310	9799.5±850	Terrestrial macrofossils

EGU

EGU
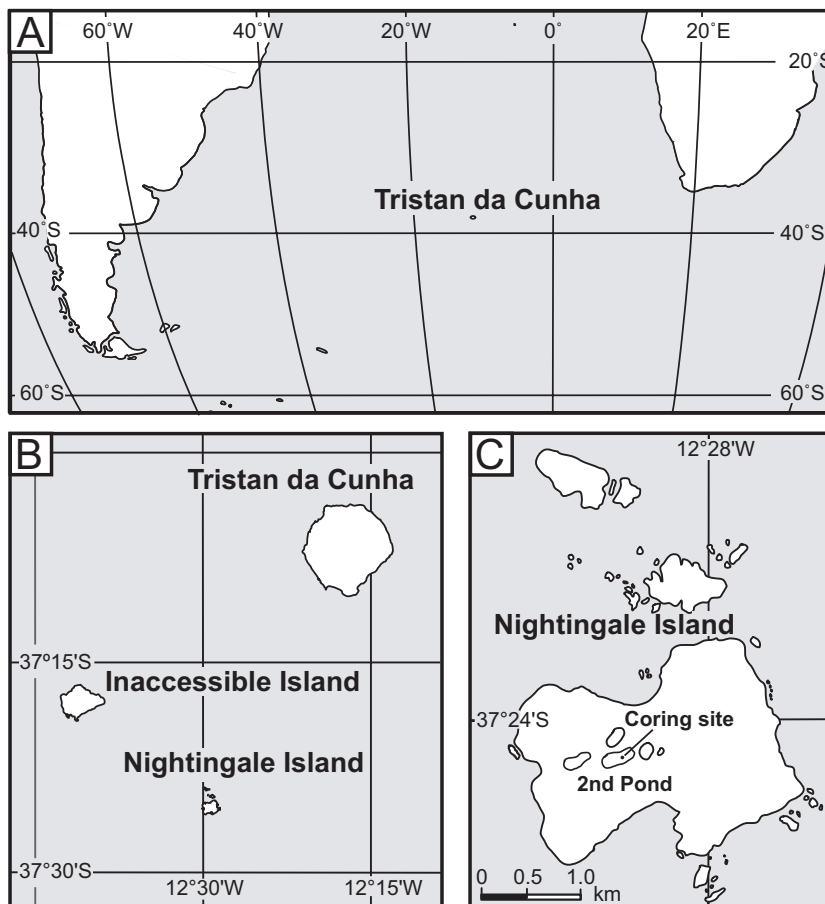
Fig. 1. (A) The position of the Tristan da Cunha island group in the South Atlantic. **(B)** The three main islands of the group. **(C)** Nightingale Island and the position of the coring site, 2nd Pond.
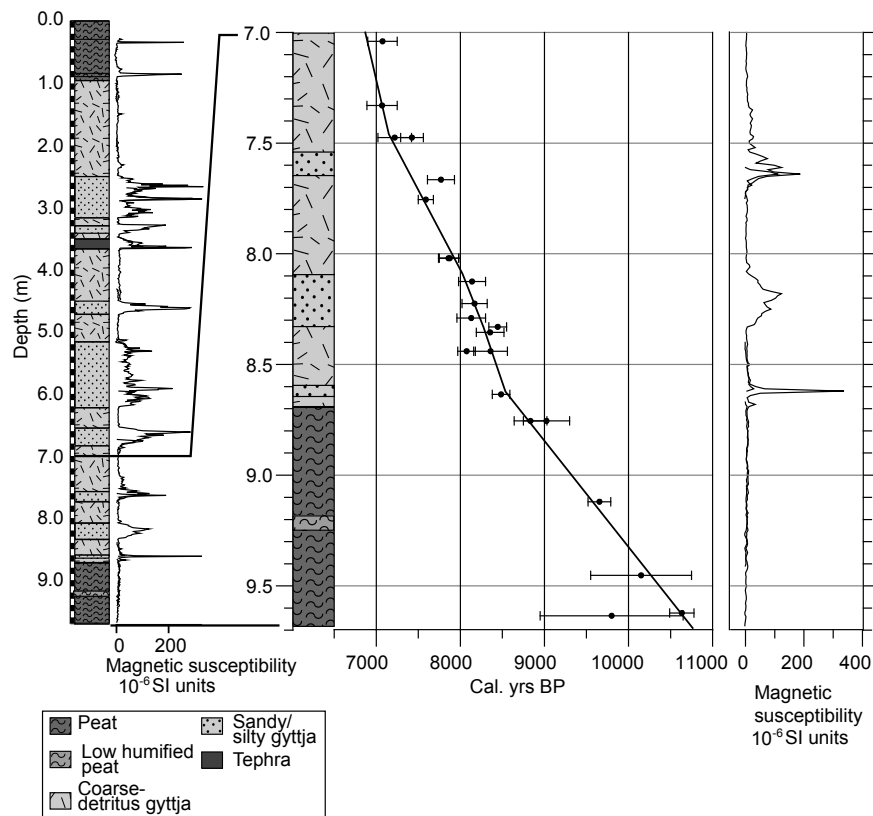
EGU

Fig. 2. Graph of lithology and susceptibility of the full 2nd Pond sediment sequence (to the left), with lithology, radiocarbon dates and magnetic susceptibility of the lowermost 2.68 m to the right. The assumed age-depth relationship is shown by the line through most of the dates and horizontal error bars denote the double standard deviation. Calendar ages are related to AD 1950.
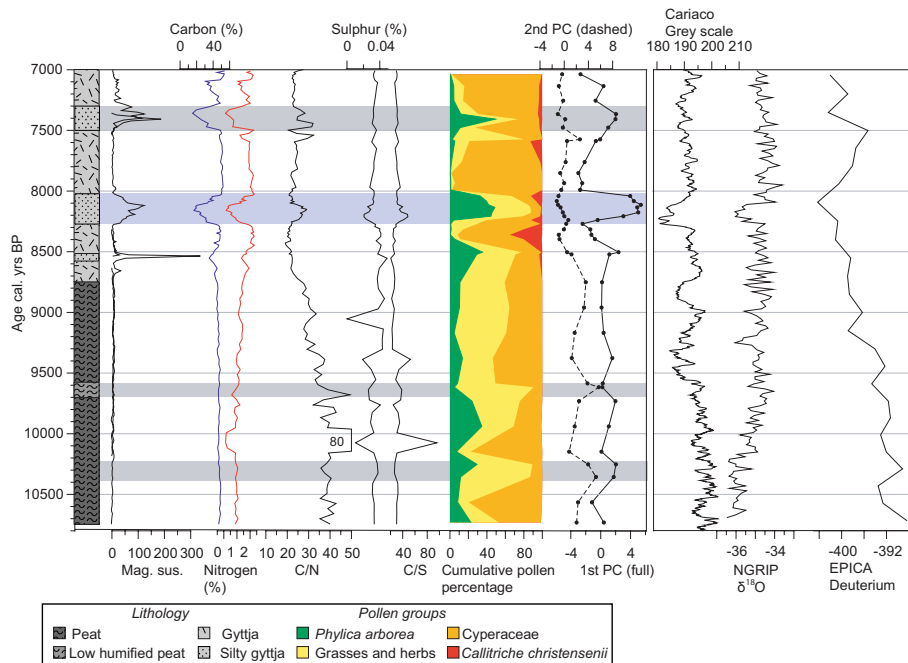
Fig. 3. Graph showing the magnetic susceptibility, content of total carbon (TC) (blue), total nitrogen (TN) (red), total sulphur content (TS), TC/TN ratios, TC/TS ratios (black), cumulative pollen percentages of *Phylica arborea* (green), grasses and herbs (yellow), sedges (orange), and *Callitriche christensenii* (red), and the values of the first two PCA axes of the pollen data set accounting for 42% of the total variance. All data are related to the age model shown in Fig. 2. The 8.2 kyr event is marked by blue color, while the other two events discussed in the text are shown by grey shading. In addition to the 2nd Pond data, the updated grayscale record from the Cariaco Basin (Haug et al., 2001), the ^{18}O values from the NGRIP ice core (Rasmussen et al., 2006), and deuterium from the EPICA ice core (Epica community members, 2004; Röthlisberger et al., 2002). The latter three have independent chronologies based on varve years and ice years BP.
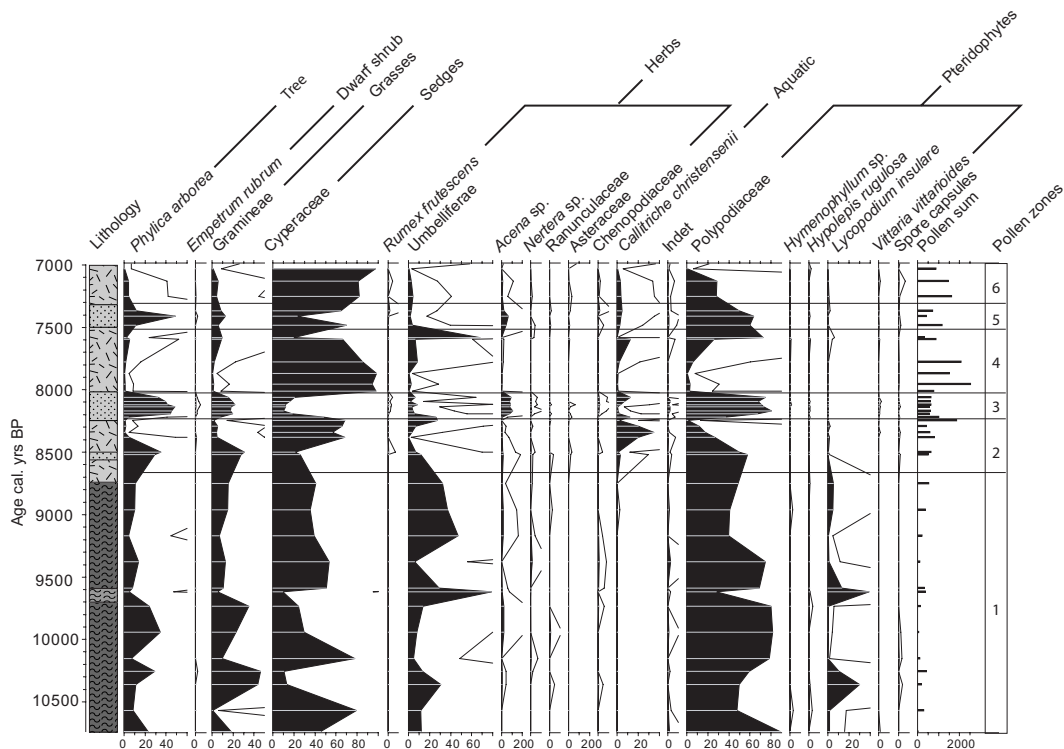
Fig. 4. Graph showing pollen percentages. Pollen percentages were calculated using all pollen types, while Pteridophyte frequencies were calculated with a combined pollen and spore sum. Pollen zonation is based on the major variation in the full pollen percentage dataset which is clearly expressed in the 1st and 2nd PCA axes. The zonation concurs with major lithological changes shown to the left.

EGU

EGU
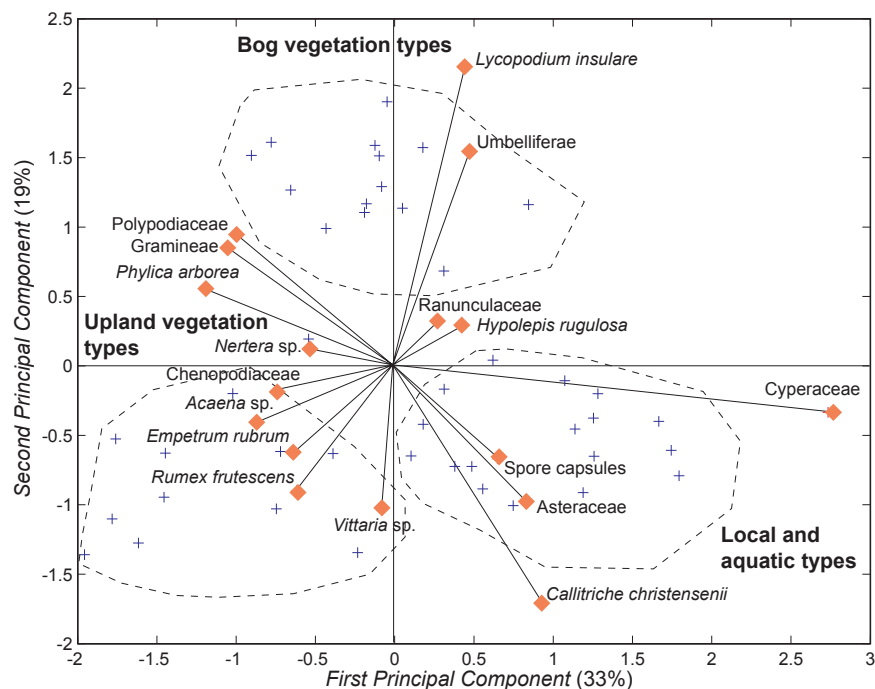
Fig. 5. Biplot of PCA variables (red diamonds), and sample scores (blue crosses). Note that the scores are scaled. Dashed lines indicate the three major sample score groupings. The variable scores show that, the upper central group is influenced by *Lycopodium insulare* and Umbeliferae, which represent the bog vegetation assemblages. The two other groups represent the period of gyttja deposition and separate between deposition of pollen from the local vegetation, samples in the lower right corner mainly influenced by Cyperaceae and *Callitriche christensenii* , and deposition of pollen from more distal parts of the catchment during periods of increased erosion, samples in the lower left corner mainly influenced by *Phylica arborea* , Polypodiaceae, *Acaena* sp., *Rumex frutescens* and *Empetrum rubrum*.
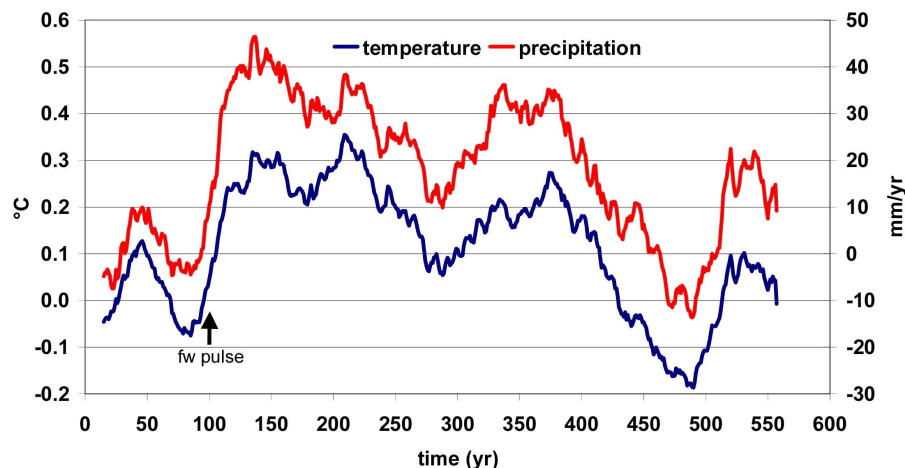
EGU

Fig. 6. Simulation of the 8.2 kyr event over the Southeast Atlantic (20° W–10° E, 40° S–20° S), shown by the response in annual mean sea surface temperature (left axis) and precipitation (right axis) to a freshwater pulse (fw pulse) in the Labrador Sea (Alley and Ágústsdóttir, 2005). Presented are the 30 year running mean anomalies relative to a reference climate in quasi-equilibrium with 8.5 kyr BP forcings (represented by the first 100 years). In the experiment, the THC of this 8.5 kyr state was perturbed by a 20 year long freshwater flux with a 0.75 Sv rate in the Labrador Sea, starting at year 100 (Alley and Ágústsdóttir, 2005; Rohling and Pälike, 2005). The THC weakening ends at year 420, followed by a ~100-year long "overshoot" during which the accumulated heat is released in the North Atlantic.